

# Preparation and characterization of gel electrolyte with bacterial cellulose coated with alternating layers of chitosan and alginate for electric double-layer capacitors

Ditpon Kotatha<sup>1</sup> · Kenta Morishima<sup>1</sup> · Satoshi Uchida<sup>1</sup> · Mayuko Ogino<sup>1</sup> · Masashi Ishikawa<sup>1</sup> · Tetsuya Furuike<sup>1</sup> · Hiroshi Tamura<sup>1</sup>

Received: 15 June 2017 / Accepted: 26 July 2017 / Published online: 24 February 2018  
© Springer Science+Business Media B.V., part of Springer Nature 2018

**Abstract** A novel gel electrolyte has been prepared using bacterial cellulose (BC) coated with chitosan (CTS) and alginate (Alg) layers, which contain 1-ethyl-3-methylimidazolium tetrafluoroborate (EMImBF<sub>4</sub>). The gel electrolyte was optimized for use in solvent-free solid-stage electric double-layer capacitors (EDLCs). The inoculated BC was oxidized and coated with alternating layers of CTS and Alg via ionic crosslinking to produce the gel electrolytes. The CTS content of the obtained gel electrolytes linearly increased with an increase in the number of CTS and Alg layers on the BC fibers. The results imply that the CTS and Alg layers successfully bound onto each BC fiber, which was consistent with Fourier transform infrared spectroscopy measurements. Based on a structural analysis, the fabricated gel electrolytes had a nanofibrous structure with a fiber diameter range of approximately 78.6–99.0 nm, a high thermal stability, and a significantly improved tensile strength compared to gel electrolytes of only CTS or Alg. In addition, EDLCs have been fabricated using the new gel electrolyte with activated carbon as the active material. The electrochemical performance of the EDLCs was determined via charge–discharge testing and alternating current impedance measurements. The EDLCs cell with a gel electrolyte of BC coated with 15 layers of CTS and Alg containing EMImBF<sub>4</sub> showed a high discharge capacitance, implying that the high affinity of this gel electrolyte for the activated carbon electrode leads to reduced electrode/electrolyte interfacial resistance, which shows the potential of this approach compared with liquid-phase EMImBF<sub>4</sub> to obtain high-performance, safety-oriented EDLCs.

**Keywords** Bacterial cellulose · Chitosan · Alginate · Gel electrolyte · Ionic liquid · Electric double-layer capacitor

---

✉ Hiroshi Tamura  
tamura@kansai-u.ac.jp

<sup>1</sup> Faculty of Chemistry, Materials and Bioengineering, Kansai University, 3-3-35 Yamate-cho, Suita, Osaka 564-8680, Japan

## Introduction

With advances in electronic technologies, there is a demand for high-energy power-storage devices to be manufactured in a compact and handy-to-use way without a reduction in their performance. Electric double-layer capacitors (EDLCs), also known as supercapacitors, can be functional and meet the abovementioned requirements. The energy storage mechanism of EDLCs arises from non-faradic phenomena between two non-faradic electrodes and an electrolyte at their interfaces [1–3]. This can provide a higher sustained power density and longer charge–discharge cycle (> 100,000 cycles) as compared with rechargeable battery systems [4, 5].

Owing to their excellent properties such as near-zero vapor pressure, high thermal stability, and non-flammability, ionic liquids (ILs), which have been widely promoted as green solvents [6–8], are being studied as electrolytes for EDLCs [9–14]. However, the liquid leakage and lack of safety associated with IL electrolytes in the EDLCs system must be considered. Hence, non-aqueous electrolytes are more promising for EDLCs. The various gel electrolytes, including IL-based electrolytes, have been prepared [15–22].

Considering depletion of nonrenewable resources, sustainable development and application of biodegradable polymers have attracted significant attention. In recent years, biomass such as carrageen [23–26], agar [27, 28], starch [29–31], and guar gum polysaccharide [32] have been developed for gel-polymer electrolytes. In addition, previous studies have reported successful preparation of gel electrolytes from chitosan (CTS) [33–35] and alginate (Alg) [35–38], including high-performance ILs for use in EDLCs. However, the low tensile strength of these gel electrolytes may be attributed to the properties of the materials used.

Bacterial cellulose (BC), which is natural polymer nanofiber, displays unique physical and chemical properties such as good biocompatibility, high water absorption capacity, high crystallinity, highly fibrous networks, and a high tensile strength and modulus [39, 40]. Therefore, if BC is used as the scaffold for CTS and Alg as a gel electrolyte, it is possible to efficiently combine both the higher tensile strength and the electrochemical properties of these materials.

In this work, a novel gel electrolyte was successfully prepared using BC coated with alternating layers of CTS and Alg including 1-ethyl-3-methylimidazolium tetrafluoroborate (EMImBF<sub>4</sub>) for the use in EDLCs. The characterization of the gel electrolyte and its electrochemical properties are discussed.

## Experimental

### Materials

*Gluconacetobacter xylinus* ATCC 53582 was purchased from Summit Pharmaceuticals International Corporation (Japan). Chitosan [FL-80, Mw 90,000, degree of deacetylation (DDA): 89.7%] and sodium Alg (viscosity: 80–120 mPa s for 10 g/L at 20 °C) were supplied from Koyo Chemical Co., Ltd. (Japan) and KIMICA

Corporation (Japan), respectively. 1-ethyl-3-methylimidazolium tetrafluoroborate (EMImBF<sub>4</sub>, 99.0%) was purchased from Toyo Gosei Co., Ltd. (Japan). Activated carbon (YP-50F), acetylene black (HS-100), sodium carboxymethyl cellulose (WS-C), and styrene-butadiene rubber (TRD2001) were purchased from Kuraray Co., Ltd. (Japan), Denka Company Ltd. (Japan), DKS Co., Ltd. (Japan), and JSR Corporation (Japan), respectively. Other reagents were purchased from Wako Pure Chemical Company (Japan) and used without further purification.

## Preparation of gel electrolytes of BC coated with alternating layers of CTS and Alg

### *Preparation of BC gel*

The starting culture of *Gluconacetobacter xylinus* was inoculated at 30 °C for 7 days with 1 mL of *Gluconacetobacter xylinus* in 200 mL of Hestrin–Schramm (HS) medium containing 2% D-glucose, 0.5% yeast extract, 0.5% peptone, 0.115% sodium hydrogen phosphate, and 0.27% citric acid in deionized (DI) water (w/v) [41, 42]. The HS medium was sterilized at 121 °C for 15 min before use [43]. After the incubation period, BC was cultured at room temperature for 3 days by adding 1 mL of starter culture in 20 mL of HS medium. Subsequently, the obtained BC gel was washed with DI water to remove the HS medium and was treated in a 0.5 M sodium hydroxide (NaOH) solution at 90 °C for 1 h to eliminate bacterial cells [40]. Then, the treated BC gel was washed with DI water until the pH of the filtrate was neutral before using the gel in future processes.

### *Preparation of BC coated with alternating layers of CTS and Alg*

The BC nanofiber was oxidized with potassium periodate (KIO<sub>4</sub>) before coating it with CTS and Alg. The BC was submerged in 400 mL of a 1-mg/mL KIO<sub>4</sub> solution and was stirred at 60 °C for 1 h [44]. The oxidized BC was then washed with DI water several times to remove the KIO<sub>4</sub>; then, it was soaked in DI water overnight at room temperature before coating with CTS and Alg in the next step.

The oxidized BC was coated layer by layer with CTS and Alg as follows: The CTS and Alg solutions were prepared with a concentration of 0.1% (w/v). The CTS solution was prepared by adding 0.4 g of CTS powder to 2% (v/v) aqueous acetic acid to a volume of 400 mL and by subsequent stirring at 60 °C for 1 h. Meanwhile, the Alg solution was prepared by adding 0.4 g of Alg powder to DI water to a volume of 400 mL and by subsequent stirring at 60 °C for 1 h. Subsequently, the oxidized BC was submerged in 400 mL of 0.1% (w/v) CTS solution and stirred at 60 °C for 1 h to coat it with a layer of CTS. Then, the CTS-coated oxidized BC was submerged in 400 mL of 0.1% (w/v) Alg solution and stirred at 60 °C for 1 h to coat it with a layer of Alg. Accordingly, the sample was coated with additional CTS layers alternated with Alg layers. The coated sample was washed in 400 mL of DI water in an ultrasonic machine twice before repeated CTS or Alg coatings. The number of coating layers of CTS alternated with Alg on the samples were 5, 10, and 15. The corresponding products were labelled as BC/(CTS/Alg)<sub>5</sub>, BC/(CTS/Alg)<sub>10</sub>,

and BC/(CTS/Alg)<sub>15</sub>, respectively. After coating, the sample thickness was reduced via pressing with a 2-kg load for 2 h, and the thickness of the obtained samples was restrained up to approximately 100 μm; then, it was soaked in 400 mL of methanol for 3 days; the methanol bath was changed every day. The sample thus obtained was used in the subsequent steps.

## Characterization of gel electrolyte

### Fourier transform infrared spectroscopy (FTIR)

FTIR (670-IR, VARIAN Inc., USA) was used for identifying the functional groups in the obtained samples.

### Determination of CTS content

The CTS content in the obtained samples was determined via the Kjeldahl method [45, 46]. The sample was dried at 50 °C overnight; then, it was vacuum-dried at room temperature overnight before analysis. First, the digestion process was performed as follows: Approximately 100 mg of the sample was digested with 10 mL of concentrated sulfuric acid in the presence of 3 g of catalyst (9:1 ratio of potassium sulfate-to-copper sulfate) and 5 mL of 35% (v/v) hydrogen peroxide in a digestion tube at 420 °C until the digested solution became transparent. The digested solution was then cooled to room temperature, and distillation and titration were performed as follows: The digestion tube with the digestion solution was attached to the distillation unit and 30% (w/v) of NaOH solution was added to the digestion solution until the solution turned black. Steam distillation was performed for approximately 15 min. The distilled ammonia was received into DI water (30 mL) containing 2–4 mL of 0.05 M hydrochloric acid (HCl) in an Erlenmeyer flask. A few drops of the indicator [a 0.05% (w/v) methyl red-methylene blue ethanol solution] were added to the solution before titrating the solution with a standardized 0.01 M NaOH solution. The CTS content (%) was determined using Eqs. (1) and (2):

$$M_{\text{CTS}} = M_{\text{GlcN}} \frac{\text{DDA}}{100} + M_{\text{GlcNAc}} \frac{100 - \text{DDA}}{100} \quad (1)$$

$$\text{CTS content (\%)} = \frac{M_{\text{CTS}}(C_{\text{HCl}}V_{\text{HCl}} - C_{\text{NaOH}}V_{\text{NaOH}})}{W} \times 100 \quad (2)$$

where  $M_{\text{CTS}}$  is the average molecular weight of a sugar unit of CTS and  $M_{\text{GlcN}}$  and  $M_{\text{GlcNAc}}$  are the molecular weights of a glucosamine unit and an *N*-acetyl-glucosamine unit, respectively.  $C$  (g/1000 mL) and  $V$  (mL) denote the concentrations and volumes of HCl and NaOH, respectively.  $W$  (g) is the total weight of the tested sample.

### Scanning electron microscopy (SEM)

SEM (JSM6700, JEOL, Japan) was used to analyze the morphology of the obtained samples at an accelerating voltage of 5 kV with 20-k magnification. The diameter-

size distribution of the BC nanofibers was analyzed based on the SEM images using image visualization software.

### *Porosity*

Porosity of the sample was determined using liquid displacement according to previous literature [47]. Ethanol was used as the displacing liquid. The sample dimensions were measured using a Vernier caliper, and the volume was calculated. The sample was freeze-dried and soaked in ethanol for 24 h to allow the ethanol to penetrate into the pores of the sample. The weight of the sample before and after soaking in ethanol was measured. The porosity (%) of the sample was determined using Eq. (3)

$$\text{Porosity (\%)} = \frac{(W_f - W_i)}{\rho_{\text{ethanol}} \times V} \times 100 \quad (3)$$

where  $W_f$  (g) is the weight of the dry sample,  $W_i$  (g) is the weight of the wet sample after soaking in ethanol,  $\rho_{\text{ethanol}}$  (0.789 g/cm<sup>3</sup>) is the density of ethanol, and  $V$  (cm<sup>3</sup>) is the volume of the sample.

### *Thermogravimetric analysis (TGA)*

A thermogravimetric/differential thermal analyzer (EXSTAR TG/DTA 6200, SII, Japan) was used to analyze the thermal properties of the obtained samples. All samples were vacuum-dried at room temperature for 2 days before analysis. The samples were measured at a heating rate of 20 °C/min in the range of 25–600 °C in a nitrogen atmosphere.

### *Determination of mechanical properties*

The mechanical properties of the obtained samples were determined using a universal testing machine (STA-1150, A&D Company, Ltd., Japan) equipped with a 50-N load cell at a constant speed of 10 mm/min in ambient conditions. The sample was cut to a size of 30 mm in length and 5 mm in width, was mounted in tensile grips before the analysis, and was measured more than 10 times. Tensile parameters, including tensile strength and elongation at break, were determined from the stress–strain curves obtained from the force–distance data.

### **Fabrication of EDLC cells**

The BC, BC/(CTS/Alg)<sub>5</sub>, BC/(CTS/Alg)<sub>10</sub>, and BC/(CTS/Alg)<sub>15</sub> samples were cut into 16-mm diameter disks and immersed in EMImBF<sub>4</sub>. The immersed samples were then vacuumed under 0.3 Pa at room temperature for 48 h to remove impurities such as methanol and moisture. The thicknesses of the obtained gel electrolytes were approximately 100 μm.

An activated carbon composite electrode for a test cell was prepared via the following process. Activated carbon, acetylene black (as a conductive additive),

1.2% (w/w) sodium carboxymethyl cellulose (as a dispersant), and 48% (w/w) styrene-butadiene rubber (as a binder) were homogeneously dispersed in DI water with a weight ratio of 90:5:3:2. The obtained electrode slurry was cast onto an etched aluminum current collector and dried, and the obtained composite electrode sheet was cut into 12-mm diameter disks.

A pair of activated carbon electrodes was immersed in EMImBF<sub>4</sub> for 10 min under a vacuum before assembling the test cells. Two-electrode coin cells were assembled using this pair of electrodes and a gel electrolyte (one of the samples described previously) for electrochemical measurements. A test cell containing EMImBF<sub>4</sub> as a liquid electrolyte with a cellulose separator (TF4035, Nippon Kodoshi Corporation, Japan) was also fabricated for comparison. All assembly procedures were conducted in an argon-filled glove box.

## Electrochemical measurement

The performances of these EDLC test cells were measured using a battery charge–discharge apparatus (HJ1001 SM8, Hokuto Denko Corporation, Japan). The charge–discharge tests were conducted with a voltage range of 0–2.5 V at several current densities in the range of 2.5–100 mA/cm<sup>2</sup>. The discharge rate performance of the EDLCs at various discharge current densities was also estimated after applying a constant current charge up to 2.5 V. The discharge capacitance of a single electrode in the present EDLC symmetrical cells was determined using Eq. (4):

$$C = \frac{I \times t}{(V/2) \times W} \quad (4)$$

where  $C$  (F/g) is the discharge capacitance,  $I$  (A) is the discharge current,  $t$  (s) is the discharge time,  $V$  (V) is the operating voltage, and  $W$  (g) is the mass loading of activated carbon at a single electrode [35–38]. Alternating current (AC) impedance of the test cells was measured using a potentiogalvanostat (SI 1287 type, Solartron Analytical, UK) and frequency response analyzer (SI 1260 type, Solartron Analytical, UK). The AC amplitude was 10 mV<sub>p-0</sub> and the frequency range was 500 kHz–10 mHz. All of the electrochemical measurements were carried out at 25 °C.

## Results and discussion

### Characterization of gel electrolyte

#### *Determination of CTS content*

The CTS content (%) in the BC of several samples after coating with alternating layers of CTS and Al<sub>2</sub>O<sub>3</sub> is shown in Fig. 1. The results show that the CTS content linearly increased ( $R^2 = 0.999$ ) when the number of CTS layers on the BC increased, implying that the layers of CTS and Al<sub>2</sub>O<sub>3</sub> bound to each BC fiber. A schematic of the coating process is shown in Fig. 2.

## FTIR

The FTIR spectra of BC and BC coated with alternating layers of CTS and Alg are shown in Fig. 3. All samples showed absorption peaks in the region  $3600\text{--}3000\text{ cm}^{-1}$ ; these correspond to the stretching vibrations of O–H groups and peaks at approximately  $2900\text{ cm}^{-1}$ , which are induced by the stretching vibration of  $\text{CH}_2$ . The various peaks in the  $1450\text{--}1200\text{-cm}^{-1}$  region are due to the stretching of C–H, and the peaks at about  $1060$  and  $1035\text{ cm}^{-1}$  are due to the stretching of C–O–C. These absorption peaks are characteristic of BC, while the absorption peak at  $1640\text{ cm}^{-1}$  is related to the H–O–H bending vibration of water absorbed in the material [48, 49].

Owing to the small percentage of CTS and Alg on the BC fiber, the FTIR spectrum of BC coated with alternating layers of CTS and Alg is very similar to that of the BC. However, the most obvious difference between their FTIR spectra is the slight shift of the broad peak for the O–H and N–H groups of BC/(CTS/Alg)<sub>5</sub>, BC/(CTS/Alg)<sub>10</sub>, and BC/(CTS/Alg)<sub>15</sub> compared with the peaks seen in normal BC in the ranges of  $3370\text{--}3400$  and  $3430\text{--}3457\text{ cm}^{-1}$ , respectively. The increase in the CTS content on the BC fiber after coating with alternating layers of CTS and Alg indicates that an increased amount of amine groups or nitrogen atoms from the CTS layer were incorporated into the BC matrix and they interacted with the O–H group in the BC fiber [50]. Moreover, the peak at approximately  $1420\text{ cm}^{-1}$  in the coated BC was stronger with a higher intensity than the same peak seen in BC because of the additional vibration from the  $\text{NH}_3^+$  group of CTS interacting with the  $\text{COO}^-$  group of Alg [51]. Further, the peak at  $1736\text{ cm}^{-1}$  was not found in the spectrum of the coated BC because there were no non-ionized COOH groups. These spectra confirmed that the carboxylate groups of sodium Alg were dissociated to  $\text{COO}^-$ , which formed complexes with the protonated amino groups of CTS via electrostatic

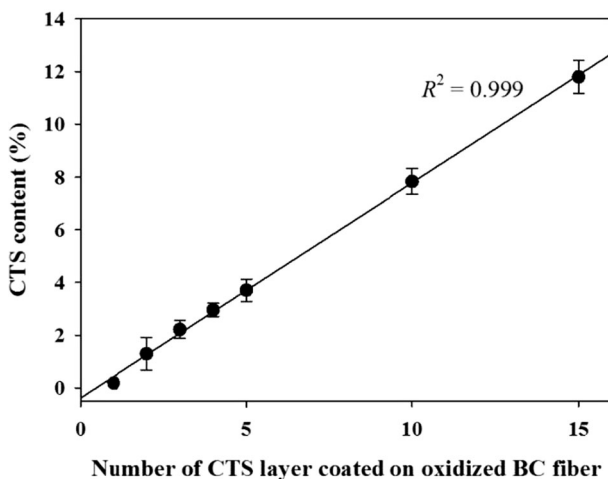


**Fig. 1** CTS content in the BC coated with alternating layers of CTS and Alg

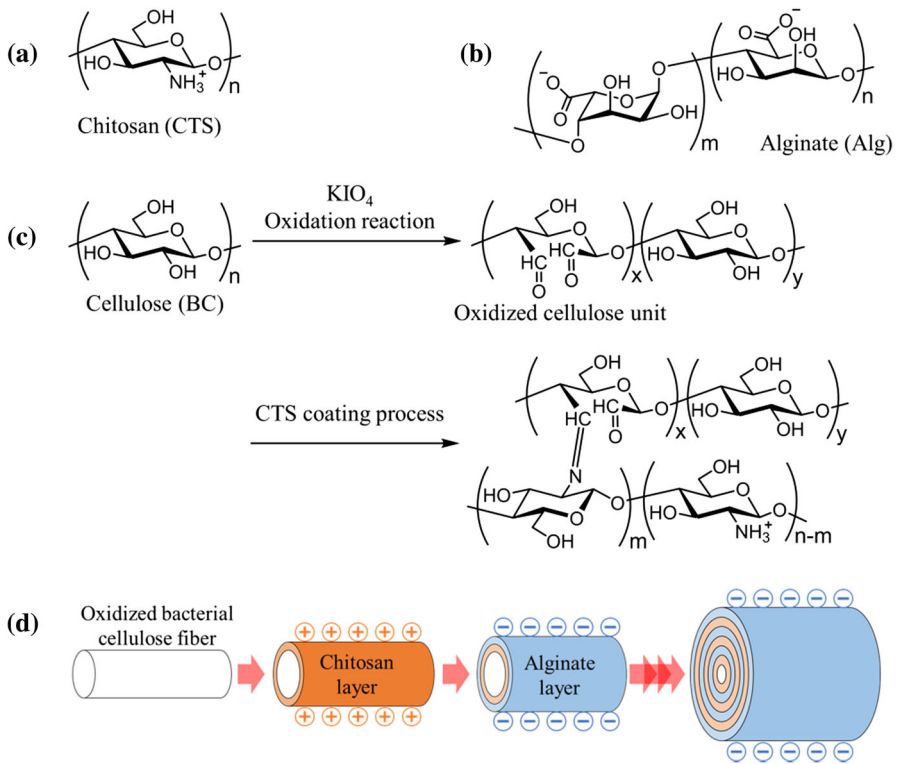


**Fig. 2** Schematic of the process for coating CTS and Alg layers on BC: **a** CTS structure, **b** Alg structure, **c** cellulose oxidation reaction and CTS coating process on BC, and **d** layer-by-layer coating process with CTS and Alg

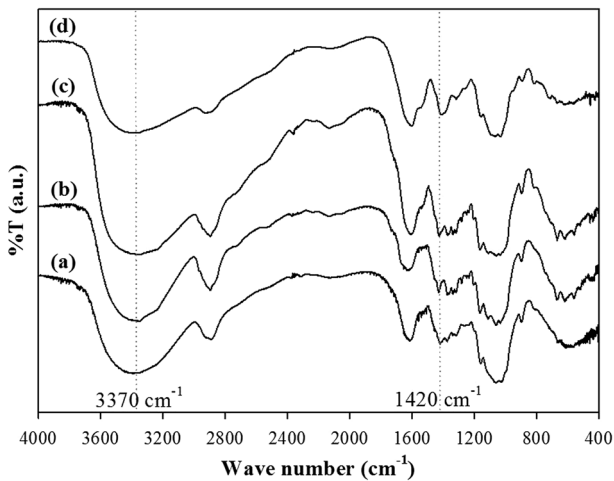


**Fig. 3** Fourier transform infrared spectroscopy spectra of **a** BC, **b** BC/(CTS/Alg)<sub>5</sub>, **c** BC/(CTS/Alg)<sub>10</sub>, and **d** BC/(CTS/Alg)<sub>15</sub>



interactions [52]. This result supports the measured CTS content results, which showed that CTS and Alg layers successfully bound on the BC fiber.

### SEM

SEM images and the measured diameter-size distribution from the SEM images of BC and coated BC are shown in Fig. 4. SEM images of BC (Fig. 4a) revealed a nanofibrous structure with an average fiber diameter of 76.8 nm, which is similar to the diameter reported in previous studies of BC [53, 54]. The diameter sizes of coated BC samples, BC/(CTS/Alg)<sub>5</sub>, BC/(CTS/Alg)<sub>10</sub>, and BC/(CTS/Alg)<sub>15</sub> were 78.1, 96.3, and 99.0 nm, respectively. The diameter size increased with an increase in the number of coating layers of CTS and Alg bound on each fiber of BC, which is consistent with the results of the CTS content and FTIR characterization.

### Porosity

The porosities at the swelling stage of BC, BC/(CTS/Alg)<sub>5</sub>, BC/(CTS/Alg)<sub>10</sub>, and BC/(CTS/Alg)<sub>15</sub> were 93.5, 89.9, 88.1, and 83.3%, respectively. The porosity of the obtained samples decreased with an increase in the number of CTS and Alg layers coated onto the BC fiber. This result suggests that the porosity of the BC gel decreased with the increase of the diameters of BC fibers, as indicated by the SEM images.

### TGA

The TGA and differential TGA (DTGA) curves of BC, coated BC, CTS powder, and sodium Alg powder are shown in Fig. 5. The CTS and sodium Alg powder had degradation temperatures at 305 and 240 °C due to the decomposition of CTS [55] and sodium Alg [56], respectively. BC and coated BC demonstrated a weight loss due to evaporation of the volatile content between 30 and 130 °C; the amount of this evaporated volatile content increased in the coated BC compared to BC. The BC sample showed merely one step of degradation at approximately 360 °C owing to the dehydration and the decomposition of cellulose molecules [57, 58]. The coated BC showed two steps of degradation; the first degradation step occurred in the range of 180–270 °C, which is in the same range as that of the degradation of sodium Alg and CTS, and it is therefore possible that this observation is due to the complex degradation process of Alg and CTS; the second step of degradation occurred in the range of 360–380 °C, which is similar to the degradation observed in BC due to dehydration and decomposition of cellulose molecules. Therefore, the results further demonstrated that the process of coating layers of CTS and Alg on the BC fiber was successful.

In addition, all obtained samples of coated BC showed high thermal stability; therefore, this material has potential to be used as gel electrolyte in EDLCs at high operating temperatures.

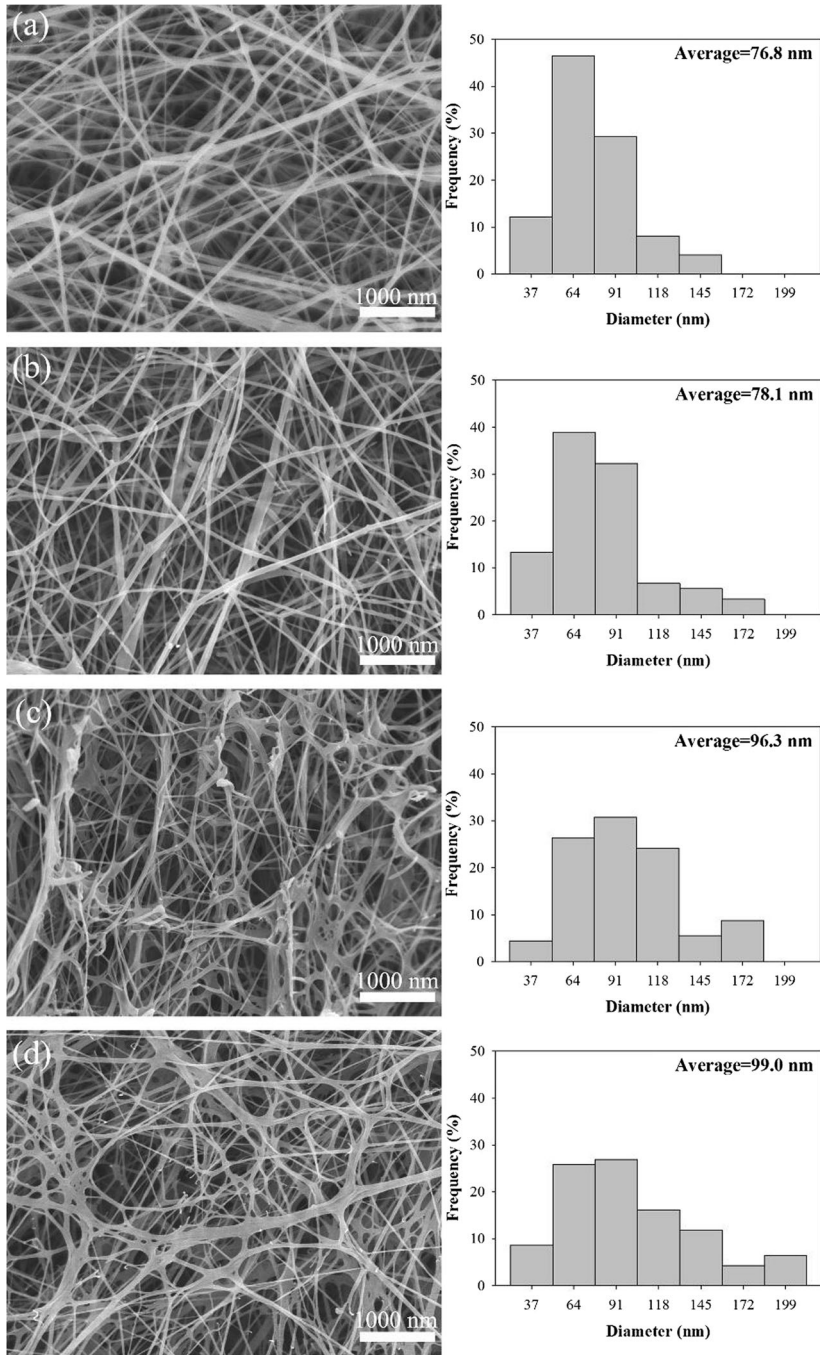


**Fig. 4** Scanning electron microscopy images and the measured diameter-size distribution of **a** BC, **b** BC/(CTS/Alg)<sub>5</sub>, **c** BC/(CTS/Alg)<sub>10</sub>, and **d** BC/(CTS/Alg)<sub>15</sub>

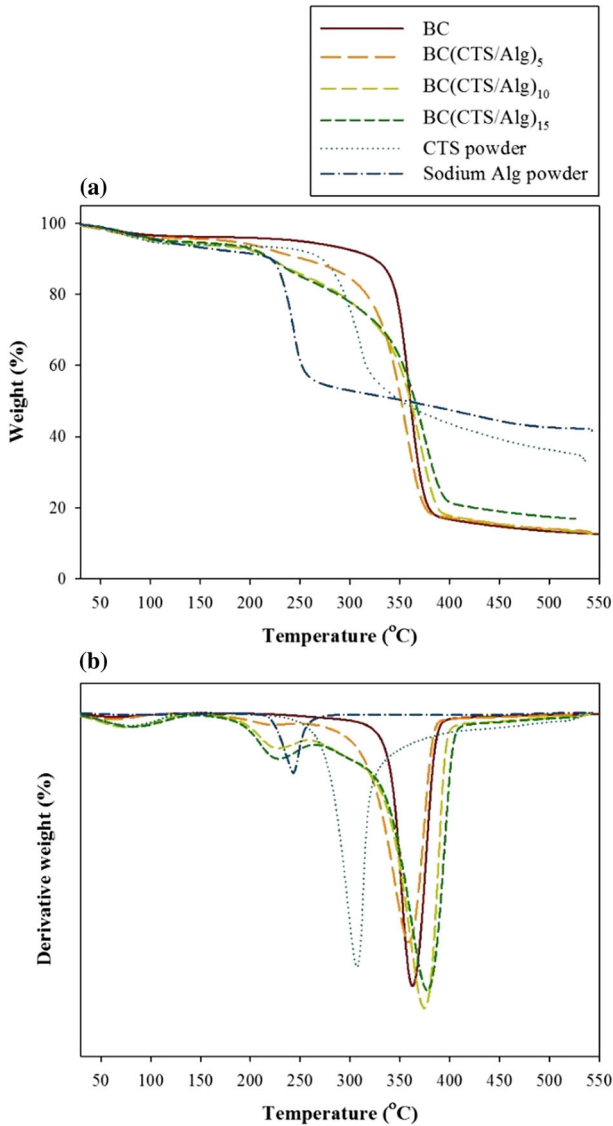


**Fig. 5** **a** TGA and **b** DTGA curves of BC, BC coated with alternating layers of CTS and Alg, CTS powder, and sodium Alg powder

### *Mechanical properties*

The mechanical properties of BC and coated BC are shown in Table 1. The CTS and Alg gel electrolytes for EDLCs were prepared for comparison of their mechanical properties [33–38]. The mechanical properties of all samples were measured at the water swelling stage. Results showed that the BC had tensile strength as high as 5.4 N, and its tensile strength increased with an increase in the

**Table 1** Tensile strength and elongation at break of various samples

Sample	Tensile strength (N)	Elongation at break (%)
BC	5.38 ± 1.09	42.21 ± 5.92
BC(CTS/Alg) <sub>5</sub>	4.48 ± 0.40	52.85 ± 8.07
BC(CTS/Alg) <sub>10</sub>	5.52 ± 0.86	33.38 ± 4.75
BC(CTS/Alg) <sub>15</sub>	8.96 ± 2.28	39.47 ± 5.43
CTS gel	0.47 ± 0.06	72.05 ± 8.70
Alg gel	0.01 ± 0.00	38.63 ± 5.67

number of CTS/Alg coating layers, which was possibly caused by the increasing fiber–fiber interaction within the sample. Considering the increase in fiber size that was observed with the increase in the number of CTS/Alg layers as seen in the SEM images, a decrease in the distance between fibers in a sample may cause the observed increase in the fiber–fiber interactions. Moreover, the tensile strengths of all gel electrolyte samples made with BC and coated BC were significantly higher than those of the gel electrolyte made with CTS/Alg. It should be noted that BC is used as a scaffold for the CTS and the Alg layers to improve the tensile strength of the resulting gel electrolyte.

On the contrary, the elongation at break was consistent in both the BC and the coated BC with an average elongation of approximately 42%, which is lower than that of the gel electrolyte made from CTS and Alg and which likely arises from the fibrous structure of the material.

## Electrochemical results

The charge–discharge curves of the EDLC test cells assembled with either the liquid-phase EMImBF<sub>4</sub> or the BC gel electrolyte with EMImBF<sub>4</sub> (BC/EMImBF<sub>4</sub>) collected at current densities of 2.5 and 50 mA/cm<sup>2</sup> are shown in Fig. 6a, b, respectively. During the 2.5-mA/cm<sup>2</sup> charge–discharge cycle, both cells showed ideal triangular charge–discharge voltage profiles, like those of typical EDLCs. On the contrary, in the charge–discharge curves measured at 50 mA/cm<sup>2</sup>, the test cell with the BC/EMImBF<sub>4</sub> gel electrolyte showed an IR drop twice as large as the test cell with liquid-phase EMImBF<sub>4</sub>. This result indicates that the BC/EMImBF<sub>4</sub> gel electrolyte had a higher resistance than that of the EMImBF<sub>4</sub>.

To improve the poor rate of performance of the BC gel electrolyte system, the 5-, 10-, and 15-layer CTS- and Alg-coated BC gel electrolytes, including EMImBF<sub>4</sub> [BC/(CTS/Alg)<sub>5</sub>/EMImBF<sub>4</sub>, BC/(CTS/Alg)<sub>10</sub>/EMImBF<sub>4</sub>, and BC/(CTS/Alg)<sub>15</sub>/EMImBF<sub>4</sub>, respectively] were prepared as gel electrolytes, which had ionic functional groups with a good affinity for ILs. The electrochemical performance of the electrolytes was investigated. The charge–discharge curves of the EDLC test cells assembled with the liquid-phase EMImBF<sub>4</sub>, BC/EMImBF<sub>4</sub>, BC/(CTS/Alg)<sub>5</sub>/EMImBF<sub>4</sub>, BC/(CTS/Alg)<sub>10</sub>/EMImBF<sub>4</sub>, or BC/(CTS/Alg)<sub>15</sub>/EMImBF<sub>4</sub> collected at high current densities of 100 mA/cm<sup>2</sup> are shown in Fig. 6c. The results showed that the EDLC test cells containing BC gel electrolytes with smaller numbers of CTS/Alg layers exhibited poor electrochemical performance. The test cell with BC/

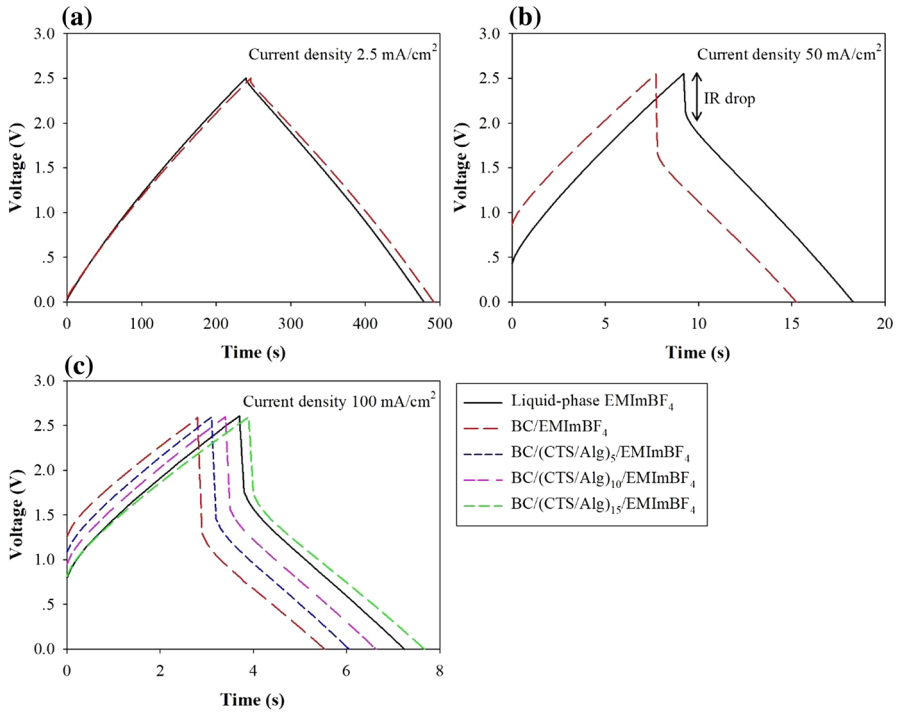


**Fig. 6** Charge–discharge curves of the EDLC test cells assembled with the liquid-phase EMImBF<sub>4</sub> or the obtained gel electrolytes, collected at current densities of **a** 2.5, **b** 50, and **c** 100 mA/cm<sup>2</sup>

EMImBF<sub>4</sub>, BC/(CTS/Alg)<sub>5</sub>/EMImBF<sub>4</sub>, and BC/(CTS/Alg)<sub>10</sub>/EMImBF<sub>4</sub> gel electrolyte systems showed a larger IR drop than the liquid-phase EMImBF<sub>4</sub> system, while the test cells with the BC/(CTS/Alg)<sub>15</sub>/EMImBF<sub>4</sub> gel electrolyte showed an improved small IR drop, similar to that observed in the liquid-phase EMImBF<sub>4</sub> system.

In addition, the discharge capacitances of the test cells assembled with the liquid-phase EMImBF<sub>4</sub> and various gel electrolytes as a function of the applied current density (2.5–100 mA/cm<sup>2</sup>) are shown in Fig. 7. The test cells with BC/EMImBF<sub>4</sub>, BC/(CTS/Alg)<sub>5</sub>/EMImBF<sub>4</sub>, and BC/(CTS/Alg)<sub>10</sub>/EMImBF<sub>4</sub> gel electrolyte showed lower discharge capacitance retention than the liquid-phase EMImBF<sub>4</sub> system, and their difference became more significant with an increase in current density, while the test cells with the BC/(CTS/Alg)<sub>15</sub>/EMImBF<sub>4</sub> gel electrolyte showed a relatively higher discharge capacitance than the test cells with the liquid-phase EMImBF<sub>4</sub> system across the entire current density range. The calculated capacitance retentions from the initial current density of 2.5–100 mA/cm<sup>2</sup> of the test cells with the liquid-phase EMImBF<sub>4</sub>, BC/EMImBF<sub>4</sub>, BC/(CTS/Alg)<sub>5</sub>/EMImBF<sub>4</sub>, BC/(CTS/Alg)<sub>10</sub>/EMImBF<sub>4</sub>, and BC/(CTS/Alg)<sub>15</sub>/EMImBF<sub>4</sub> gel electrolyte were 59.6, 45.4, 51.2, 55.7, and 60.7%, respectively. The results showed that the calculated capacitance retentions of the test cell with the BC/(CTS/Alg)<sub>15</sub>/EMImBF<sub>4</sub> system were slightly higher than liquid-phase EMImBF<sub>4</sub> system and were also comparable with the test

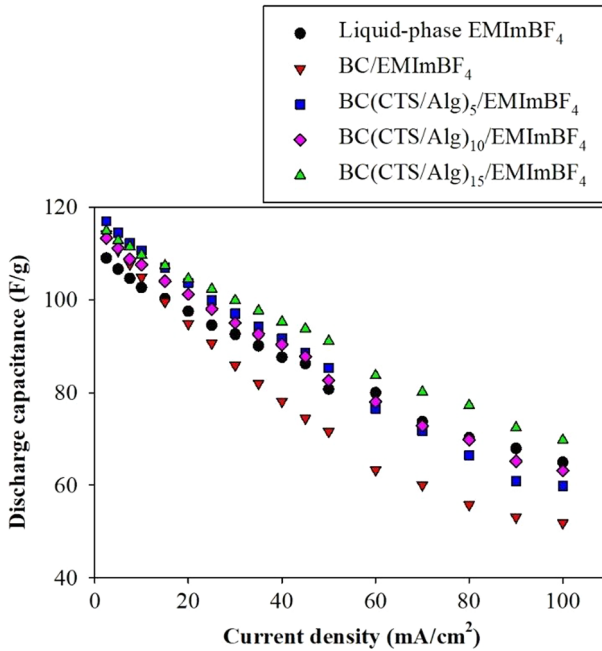


**Fig. 7** Discharge capacitances of the EDLC test cells assembled with the liquid-phase EMImBF<sub>4</sub> or the obtained gel electrolytes

cell using gel electrolyte from CTS or Alg, as shown in a previous report [34, 38], which significantly improved the tensile strength. As a result, it should be noted that the BC/(CTS/Alg)<sub>15</sub>/EMImBF<sub>4</sub> was suitable and necessary to guarantee excellent electrochemical performance of the EDLC cells.

To investigate the role of the Alg and CTS coating on BC fiber, the test cells were measured for AC impedance. The Nyquist plots of the test cells assembled with the liquid-phase EMImBF<sub>4</sub>, BC/EMImBF<sub>4</sub>, and BC/(CTS/Alg)<sub>15</sub>/EMImBF<sub>4</sub> gel electrolytes are shown in Fig. 8. The thicknesses of all gel electrolytes were larger than those of the separator in the liquid-phase EMImBF<sub>4</sub> system. Nevertheless, the resistances of the electrolyte bulk, which correspond to the distance from the origin to the first intercept on the real axis, were similar for all the tested electrolyte systems ( $\sim 1 \Omega \text{ cm}^2$ ). Therefore, it can be concluded that the differences in rate performance do not arise from the bulk properties or thickness of the gel electrolytes. Conversely, there are considerable differences in the magnitudes of the semicircular components, which represent the contact resistance between an electrode and electrolyte [38, 59]; the observed semicircle of the test cell with BC/EMImBF<sub>4</sub> was about two times larger than that of the test cell with liquid-phase EMImBF<sub>4</sub>. This proves the BC fiber was in poor contact with the activated carbon, which lead to a large IR drop, as shown in charge–discharge measurements. In contrast, the BC/(CTS/Alg)<sub>15</sub>/EMImBF<sub>4</sub> gel electrolyte system showed a slightly smaller semicircle than that of the liquid-phase EMImBF<sub>4</sub> system due to the surface modification of the BC fibers, which was achieved by coating with CTS and Alg

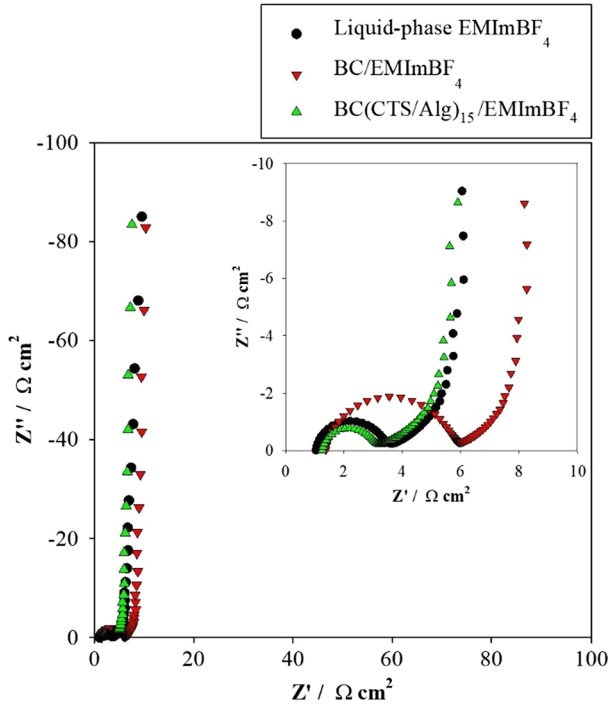


**Fig. 8** Nyquist plots obtained using AC impedance measurements of the EDLC test cells assembled with liquid-phase EMImBF<sub>4</sub>, BC/EMImBF<sub>4</sub>, or BC(CTS/Alg)<sub>15</sub>/EMImBF<sub>4</sub> gel electrolyte

layers that would facilitate better contact at the gel electrolyte/electrode interface and would accelerate ion transfer between them.

## Conclusion

In this study, a novel gel electrolyte was successfully prepared using BC coated with alternating layers of CTS and Alg for employing it as both an electrolyte and a separator in solid-state EDLCs. These gel electrolytes were produced via inoculation of the BC, oxidation in a KIO<sub>4</sub> solution, and coating with CTS layers alternated with Alg layers. As shown through analysis and characterization of the gel electrolytes, the CTS content linearly increased ( $R^2 = 0.999$ ) when the number of CTS layers on the BC increased, suggesting that the layers of CTS and Alg successfully bound onto each BC fiber. The FTIR spectra of the coated BC showed a stronger peak at  $1420 \text{ cm}^{-1}$  than unmodified BC due to the vibration of  $\text{NH}_3^+$  groups from CTS interacting with the  $\text{COO}^-$  groups of Alg. Morphological analysis based on SEM images of the obtained gel electrolyte revealed a nanofibrous structure with diameter sizes of 76.8, 78.1, 96.3, and 99.0 nm, and porosities of 93.5, 89.9, 88.1, and 83.3% for the BC, BC/(CTS/Alg)<sub>5</sub>, BC/(CTS/Alg)<sub>10</sub>, and BC/(CTS/Alg)<sub>15</sub> samples, respectively. The TGA and DTGA results revealed that all

obtained gel electrolytes had high thermal stabilities; the tensile measurement result showed very high tensile strengths in the coated BC samples as compared with the gel electrolytes made from raw CTS or Alg.

The electrochemical properties of EDLC test cells, which were assembled from the obtained gel electrolytes and carbon electrodes, were measured in terms of their charge–discharge characteristics, discharge capacitances, and AC impedance. The test cell with the BC/(CTS/Alg)<sub>15</sub>/EMImBF<sub>4</sub> gel electrolyte showed an IR drop comparable to the test cell with liquid-EMImBF<sub>4</sub> at the point of switching from charge to discharge when tested at a high current density, and a discharge capacitance higher than the test cell with liquid-phase EMImBF<sub>4</sub> across the current density range. This indicates the internal resistance of the test cell decreases when the coated BC was used as the gel electrolyte. Likewise, the AC impedance results seen in the Nyquist plot of the test cell with BC/(CTS/Alg)<sub>15</sub> represent a decrease in resistance compared with the resistance of the test cell with liquid-phase EMImBF<sub>4</sub>; this verifies that the high affinity of the proposed gel electrolyte for activated carbon electrodes can reduce the charge-transfer resistance at the electrode–electrolyte interface. The performances of the devices demonstrate that it is possible to design simple high-operating-voltage EDLCs that can replace liquid-based electrolyte systems, and thus improve the safety of such devices.

**Acknowledgements** This work was financially supported by Private University Research Branding Project, MEXT, 2016–2020, and in part by the Kansai University Outlay Support for Establishing Research Centers, 2016–2017.

## References

1. Y. Honda, M. Takeshige, H. Shiozaki, T. Kitamura, K. Yoshikawa, S. Chakrabati, O. Suekane, L. Pen, Y. Nakayama, M. Yamagata, M. Ishikawa, *J. Power Sources* **185**, 1580 (2008)
2. S. Yamazaki, T. Ito, M. Yamagata, M. Ishikawa, *Electrochim. Acta* **86**, 294 (2012)
3. S. Yamazaki, K. Obata, Y. Okuhama, Y. Matsuda, M. Yamagata, M. Ishikawa, *J. Power Sources* **195**, 1753 (2010)
4. M. Galiński, A. Lewandowski, I. Stępnia, *Electrochim. Acta* **51**, 5567 (2006)
5. M. Tokita, N. Yoshimoto, K. Fujii, M. Morita, *Electrochim. Acta* **209**, 210 (2016)
6. R.A. Sheldon, *Green Chem.* **7**, 267 (2005)
7. F. Endres, S.Z.E. Abedin, *Phys. Chem. Chem. Phys.* **8**, 2101 (2006)
8. N.V. Plechkova, K.R. Seddon, *Chem. Soc. Rev.* **37**, 123 (2008)
9. A. Lewandowski, M. Galiński, *J. Phys. Chem. Solids* **65**, 281 (2004)
10. Z. Zhou, M. Takeda, M. Ue, *J. Fluor. Chem.* **125**, 471 (2004)
11. T. Sato, G. Masuda, K. Takagi, *Electrochim. Acta* **49**, 3603 (2004)
12. K. Yuyama, G. Masuda, H. Yoshida, T. Sato, *J. Power Sources* **162**, 1401 (2006)
13. C.O. Ania, J. Pernak, F. Stefaniak, E. Raymundo-Piñero, F. Béguin, *Carbon* **44**, 3126 (2006)
14. N. Handa, T. Sugimoto, M. Yamagata, M. Kikuta, M. Kono, M. Ishikawa, *J. Power Sources* **185**, 1585 (2008)
15. M.M. Rao, J.S. Liu, W.S. Li, Y. Liang, D.Y. Zhou, *J. Membr. Sci.* **322**, 314 (2008)
16. B. Rupp, M. Schmuck, A. Balducci, M. Winter, W. Kern, *Eur. Polym. J.* **44**, 2986 (2008)
17. M. Rao, X. Geng, Y. Liao, S. Hu, W. Li, *J. Membr. Sci.* **399–400**, 37 (2012)
18. R. Prasanth, N. Shubha, H.H. Hng, M. Srinivasan, *Eur. Polym. J.* **49**, 307 (2013)
19. K. Karuppasamy, P.A. Reddy, G. Srinivas, A. Tewari, R. Sharma, X.S. Shajan, D. Gupta, *J. Membr. Sci.* **514**, 350 (2016)
20. P.F.R. Ortega, J.P.C. Trigueiro, G.G. Silva, R.L. Lavall, *Electrochim. Acta* **188**, 809 (2016)
21. M. Safa, A. Chamaani, N. Chawla, B. El-Zahab, *Electrochim. Acta* **213**, 587 (2016)



22. J. Rymarczyk, M. Carewska, G.B. Appetecchi, D. Zane, F. Alessandrini, S. Passerini, *Eur. Polym. J.* **44**, 2153 (2008)
23. N.N. Mobarak, N. Ramli, A. Ahmad, M.Y.A. Rahman, *Solid State Ionics* **224**, 51 (2012)
24. N.N. Mobarak, F.N. Jumaah, M.A. Ghani, M.P. Abdullah, A. Ahmad, *Electrochim. Acta* **175**, 224 (2015)
25. S. Rudhziah, M.S.A. Rani, A. Ahmad, N.S. Mohamed, H. Kaddami, *Ind. Crops Prod.* **72**, 133 (2015)
26. T.M.D. Palma, F. Migliardini, D. Caputo, P. Corbo, *Carbohydr. Polym.* **157**, 122 (2017)
27. E. Rapharl, C.O. Avellaneda, B. Manzolli, A. Pawlicka, *Electrochim. Acta* **55**, 1455 (2010)
28. R. Leones, F. Sentanin, L.C. Rodrigues, I.M. Marrucho, J.M.S.S. Esperança, A. Pawlicka, M.M. Silva, *Express Polym. Lett.* **6**(12), 1007 (2012)
29. A.S.A. Khair, A.K. Arof, *Ionics* **16**, 123 (2010)
30. M. Kumar, T. Tiwari, N. Srivastava, *Carbohydr. Polym.* **88**, 54 (2012)
31. M.F. Shukur, R. Ithnin, M.F.Z. Kadir, *Electrochim. Acta* **136**, 204 (2014)
32. Y.N. Sudhakar, M. Selvakumar, D.K. Bhat, *Mater. Sci. Eng. B* **180**, 12 (2014)
33. K. Soeda, M. Yamagata, S. Yamazaki, M. Ishikawa, *Electrochemistry* **81**(10), 867 (2013)
34. M. Yamagata, K. Soeda, S. Ikebe, S. Yamazaki, M. Ishikawa, *Electrochim. Acta* **100**, 275 (2013)
35. M. Yamagata, K. Soeda, S. Ikebe, S. Yamazaki, M. Ishikawa, *J. Electrochem. Soc.* **41**(22), 25 (2012)
36. M. Yamagata, K. Soeda, S. Yamazaki, M. Ishikawa, *J. Electrochem. Soc.* **25**(35), 193 (2010)
37. M. Yamagata, S. Ikebe, Y. Kasai, K. Soeda, M. Ishikawa, *J. Electrochem. Soc.* **50**(43), 27 (2013)
38. K. Soeda, M. Yamagata, M. Ishikawa, *J. Power Sources* **280**, 565 (2015)
39. Z. Wan, L. Wang, X. Yang, J. Guo, S. Yin, *Food Hydrocoll.* **61**, 269 (2016)
40. M.H. Kwak, J.E. Kim, J. Go, E.K. Koh, S.H. Song, H.J. Son, H.S. Kim, Y.H. Yun, Y.J. Jung, D.Y. Hwang, *Carbohydr. Polym.* **122**, 387 (2015)
41. S. Hestrin, M. Schramm, *Biochem. J.* **58**, 345 (1954)
42. J.K. Park, J.Y. Jung, Y.H. Park, *Biotechnol. Lett.* **25**, 2055 (2003)
43. J.H. Kim, S. Park, H. Kim, H.J. Kim, Y. Yang, Y.H. Kim, S. Jung, E. Kan, S.H. Lee, *Carbohydr. Polym.* **157**, 137 (2017)
44. X.D. Liu, N. Nishi, S. Tokura, N. Sakairi, *Carbohydr. Polym.* **44**, 233 (2001)
45. J. Junsomboon, J. Jakmunee, *Anal. Chim. Acta* **627**, 232 (2008)
46. P. Campins-Falco, S. Meseguer-Lloret, T. Climent-Santamaria, C. Molins-Legua, *Talanta* **75**, 1123 (2008)
47. B.S. Anisha, D. Sankar, A. Mohandas, K.P. Chennazhi, S.V. Nair, R. Jayakumar, *Carbohydr. Polym.* **92**, 1470 (2013)
48. G. Bali, M.B. Foston, H.M. O'Neill, B.R. Evans, J. He, A.J. Ragauskas, *Carbohydr. Res.* **374**, 82 (2013)
49. M. Ul-Islam, J.H. Ha, T. Khan, J.K. Park, *Carbohydr. Polym.* **92**, 360 (2013)
50. C. Liu, R. Bai, *J. Membr. Sci.* **267**, 68 (2005)
51. W.S.W. Ngah, S. Fatinathan, *Chem. Eng. J.* **143**, 62 (2008)
52. B. Smitha, S. Sridhar, A.A. Khan, *Eur. Polym. J.* **41**, 1859 (2005)
53. M.L. Cacicedo, M.C. Castro, I. Servetas, L. Bosnea, K. Boura, P. Tsafarakidou, A. Dima, A. Terpou, A. Koutinas, G.R. Castro, *Bioresour. Technol.* **213**, 172 (2016)
54. X. Fan, Y. Gao, W. He, H. Hu, M. Tian, K. Wang, S. Pan, *Carbohydr. Polym.* **151**, 1068 (2016)
55. I. Corazzari, R. Nistico, F. Turci, M.G. Faga, F. Franzoso, S. Tabasso, G. Magnacca, *Polym. Degrad. Stab.* **112**, 1 (2015)
56. S. Liu, Y. Li, L. Li, *Carbohydr. Polym.* **160**, 62 (2017)
57. X. Lu, X. Shen, *Carbohydr. Polym.* **86**, 239 (2011)
58. J.A. Marins, B.G. Soares, H.S. Barud, S.J.L. Ribeiro, *Mater. Sci. Eng. C* **33**, 3994 (2013)
59. A. Lewandowski, A. Swiderska, *Solid State Ionics* **161**, 243 (2003)